

Coexistence of magnetism and superconductivity in $\text{CeRh}_{1-x}\text{Ir}_x\text{In}_5$ P. G. Pagliuso,¹ C. Petrovic,^{1,2} R. Movshovich,¹ D. Hall,² M. F. Hundley,¹ J. L. Sarrao,¹ J. D. Thompson,¹ and Z. Fisk^{1,2}¹Los Alamos National Laboratory, Los Alamos, New Mexico 87545²National High Magnetic Field Laboratory, Florida State University, Tallahassee, Florida 32310

(Received 1 June 2001; published 7 August 2001)

We report a thermodynamic and transport study of the phase diagram of $\text{CeRh}_{1-x}\text{Ir}_x\text{In}_5$. Bulk superconductivity is observed over a broad range of doping, $0.3 < x \leq 1$, including a substantial range ($0.3 < x < 0.6$) over which it coexists with magnetic order (which is observed for $0 \leq x < 0.6$). The anomalous transition to zero resistance that is observed in CeIrIn_5 is robust against Rh substitution: the bulk T_c in $\text{CeRh}_{0.5}\text{Ir}_{0.5}\text{In}_5$ is more than double that of CeIrIn_5 , whereas the zero-resistance transition temperature is relatively unchanged for $0.5 < x < 1$.

DOI: 10.1103/PhysRevB.64.100503

PACS number(s): 74.70.Tx, 71.27.+a, 75.40.Cx

In conventional superconductors, magnetism and superconductivity are usually antithetical: an internal magnetic field breaks time-reversal symmetry which kills BCS superconductivity.¹ In a few cases (e.g., NdRh_4B_4 , TbMo_6S_8 , $\text{DyNi}_2\text{B}_2\text{C}$), superconductivity and magnetic order coexist, but this rare situation arises from magnetic order among localized $4f$ electrons that are uncoupled to itinerant conduction electrons which form the superconducting condensate.² In contrast, unconventional superconductivity in heavy fermion superconductors (HFS's), like the high- T_c cuprates, relies on some form of magnetic coupling to produce superconductivity.³ These HFS's appear to fall into one of two classes: those in which ordered magnetism coexists with superconductivity and those in which they compete. Most U-based HFS's belong to the first category, while the Ce-based superconductors belong to the second.⁴ For example, UPt_3 , URu_2Si_2 , UNi_2Al_3 , and UPd_2Al_3 develop superconductivity out of an antiferromagnetically ordered state that persists to $T=0$. On the other hand, the ground state of the prototypical HFS CeCu_2Si_2 can be either magnetic or superconducting depending on small (<1%) variations in stoichiometry or the application of small (<5 kbar) applied pressures.⁵ CeCu_2Ge_2 , CeRh_2Si_2 , CePd_2Si_2 , and CeIn_3 display antiferromagnetic ground states, but with the application of pressure, superconductivity can be induced when magnetism is suppressed.³ Although small windows of superconductivity can exist before magnetism is completely suppressed, this is generally attributed to "real-world" effects such as pressure and stoichiometric inhomogeneities.⁶

Here, we report a striking counterexample to the above categorization. $\text{CeRh}_{1-x}\text{Ir}_x\text{In}_5$ ($0.3 < x < 0.6$) displays superconductivity, with critical temperature $T_c \sim 1$ K over a wide range of composition, that develops out of and coexists with a magnetically ordered state, with Néel temperature $T_N \sim 4$ K. The broad range of composition over which superconductivity is observed ($0.3 < x \leq 1$) is also counter to expectation: Small amounts of chemical disorder in either U- or Ce-based HFS's are generally sufficient to destroy heavy-fermion superconductivity.⁷

CeRhIn_5 is a heavy fermion antiferromagnet ($T_N = 3.8$ K, $\gamma = 400$ mJ/mol K², where γ is the linear-in- T coefficient of heat capacity C at low temperature) in which superconductivity can be induced with applied pressure (at critical pres-

sure $P_c = 16$ kbar, $T_c = 2.1$ K, $\gamma = 400$ mJ/mol K²).^{8,9} Unlike the Ce-based materials discussed above, in CeRhIn_5 , T_N is essentially independent of pressure before disappearing, and the transition to superconductivity appears to be first order. The crystal structure in which CeRhIn_5 crystallizes is also host to two ambient-pressure heavy fermion superconductors: CeIrIn_5 ($T_c = 0.4$ K, $\gamma = 720$ mJ/mol K²),¹⁰ and CeCoIn_5 ($T_c = 2.3$ K, $\gamma = 290$ mJ/mol K²).¹¹ CeIrIn_5 displays an additional feature: it exhibits a zero-resistance transition at 1.2 K, well above the bulk T_c .¹⁰ In order to understand the unconventional magnetic behavior of CeRhIn_5 and the development of zero-resistance and bulk superconductivity in CeIrIn_5 , we have performed a detailed study of the series of isovalent alloys $\text{CeRh}_{1-x}\text{Ir}_x\text{In}_5$. Our principal results, summarized in Fig. 1, are reported below: antiferromagnetism persists for $0 < x < 0.6$ and is lost rather abruptly as a function of Ir concentration; superconductivity is observed over a broad range of doping, $0.3 < x \leq 1$, i.e., up to 70% of the Ir

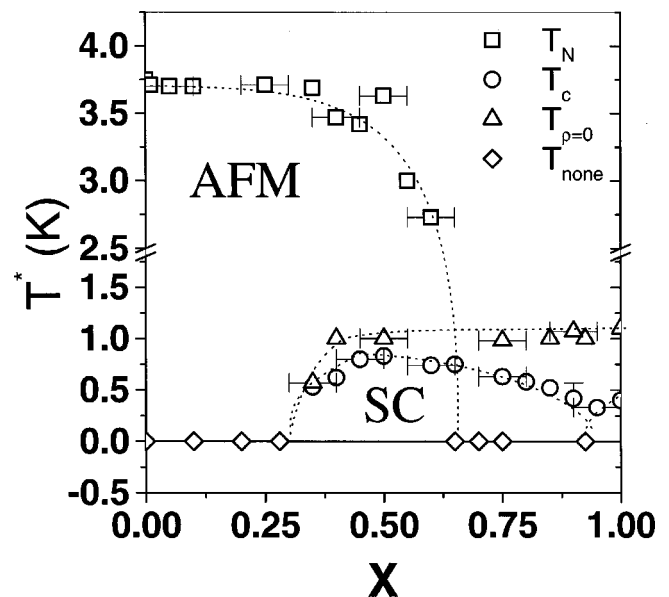


FIG. 1. Temperature-composition phase diagram of $\text{CeRh}_{1-x}\text{Ir}_x\text{In}_5$. T_{none} indicates the absence of (additional) phase transitions for $T \geq 350$ mK, the base temperature for our measurements. Lines are guides to the eye.

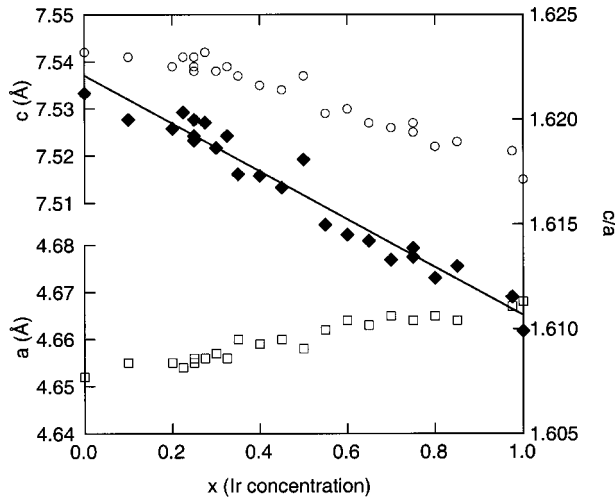


FIG. 2. Tetragonal lattice constants c (circles) and a (squares) for $\text{CeRh}_{1-x}\text{Ir}_x\text{In}_5$. The solid line is a linear fit to c/a (diamonds) as a function of x .

ions can be replaced and yet superconductivity is retained; and the separation in temperature between the zero-resistance feature and bulk superconductivity decreases with increasing Rh doping, approaching zero separation at $\text{CeRh}_{0.5}\text{Ir}_{0.5}\text{In}_5$.

Single crystals of $\text{CeRh}_{1-x}\text{Ir}_x\text{In}_5$ were grown from an In flux.⁸ Room-temperature x-ray powder diffraction measurements revealed that the materials were single phase and crystallized in the primitive tetragonal HoCoGa_5 structure.¹² In this structure, $\text{CeRh}_{1-x}\text{Ir}_x\text{In}_5$ can be viewed as layers of CeIn_3 stacked along the c axis with intervening layers of “ $\text{Rh}_{1-x}\text{Ir}_x\text{In}_2$.” No superlattice peaks at, e.g., $x = \frac{1}{2}$ were observed. Lattice constants of $\text{CeRh}_{1-x}\text{Ir}_x\text{In}_5$ are shown in Fig. 2. The a lattice constant, which is the nearest-neighbor Ce-Ce spacing in this structure, expands with increasing x , while the c axis shrinks.¹² To the extent that the measured lattice constants follow Vegard’s law, taking x as the nominal Rh:Ir ratio of the starting constituents, the nominal composition agrees well with the actual composition. From these data, we estimate an uncertainty in x of ± 0.05 at a given composition, a variation consistent with independent estimates from analysis of high-temperature magnetic susceptibility data and in crystal-to-crystal variations in ground-state properties. However, the value of x in a given crystal is always well defined; we observe no evidence for concentration inhomogeneity or phase segregation as judged by the sharpness of diffraction peaks and the low values for residual resistivity [$\rho(T \rightarrow 0) < 10 \mu\Omega \text{ cm}$ for all x] that are observed across the series, as well as the sharpness of the phase transitions observed in a given crystal.

In Fig. 3 we show C/T and magnetic entropy S as a function of T for representative x . Although the ground state changes from antiferromagnetic ($x < 0.3$) to superconducting coexisting with antiferromagnetism ($0.3 < x < 0.6$) to superconducting ($x > 0.6$), the total magnetic entropy evolved by 6 K is nearly independent of x . This indicates that the same heavy electrons are producing the variety of observed ground states and, in particular, the coexisting magnetic order and

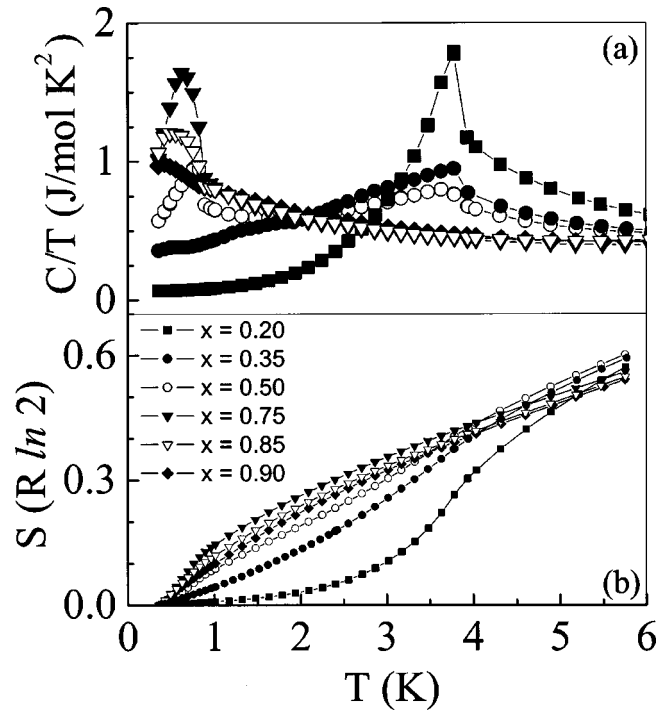


FIG. 3. Representative heat capacity divided by temperature (a) and magnetic entropy (b) versus temperature for $\text{CeRh}_{1-x}\text{Ir}_x\text{In}_5$.

superconductivity where it is observed. In the following, we discuss each of these ranges in greater detail.

For low x ($x < 0.3$), a single phase transition is observed in heat capacity whose shape and character is similar to that of stoichiometric CeRhIn_5 , in which antiferromagnetic order with $Q = (\frac{1}{2}, \frac{1}{2}, 0.297)$ develops below T_N .^{13,14} The onset of order is sharp in temperature, although the magnitude of the heat-capacity step decreases with increasing x , and the residual heat capacity below the transition is low. The independence of T_N on x is anomalous and is reminiscent of the pressure independence of T_N in CeRhIn_5 .⁸ The relative insensitivity of T_N to “out-of-plane” doping contrasts to “in-

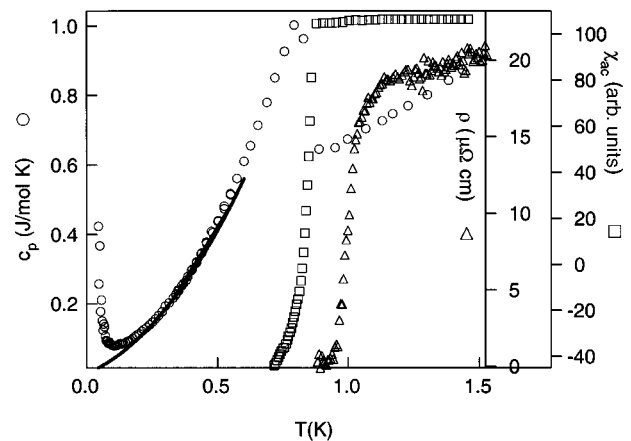


FIG. 4. Electrical resistivity, ac susceptibility, and heat capacity as a function of temperature for $\text{CeRh}_{1-x}\text{Ir}_x\text{In}_5$. The solid line is $C = 0.3 T + 1.05 T^2$, a temperature dependence similar to that observed in CeIrIn_5 (Ref. 16).

plane” doping with La in $\text{Ce}_{1-y}\text{La}_y\text{RhIn}_5$, where T_N decreases smoothly with increasing x and vanishes for $x \sim 0.4$.¹⁵

For $0.3 < x < 0.6$, T_N varies more dramatically with x , the magnetic transition broadens, and a second heat-capacity transition is observed in the vicinity of 1 K. $\text{CeRh}_{0.5}\text{Ir}_{0.5}\text{In}_5$ is the most heavily studied representative of this doping range, and heat capacity, ac susceptibility, and resistivity data are shown in Fig. 4. ac susceptibility measurements reveal that the 0.8-K transition in $\text{CeRh}_{0.5}\text{Ir}_{0.5}\text{In}_5$ is to a superconducting state (with 100% of full-shielding diamagnetism observed at the transition—as estimated based on measurements on a comparably sized and shaped sample of Sn). The jump in heat capacity at the transition $\Delta C/\gamma T_c$ is of order 1, a value comparable to that observed in stoichiometric CeIrIn_5 .¹⁰ The temperature dependence of C below T_c is also similar to that observed in CeIrIn_5 ,¹⁶ suggesting that the nature of the unconventional superconducting gap is unchanged by the coexisting magnetic state. Preliminary muon spin rotation measurements on $\text{CeRh}_{0.5}\text{Ir}_{0.5}\text{In}_5$ reveal a static contribution to the magnetization developing below 3.8 K that is similar to that observed in CeRhIn_5 and persists to 100 mK.¹⁷ These observations strongly suggest that superconductivity coexists microscopically with the ordered magnetic state. As will be discussed in more detail below, zero resistivity is observed in the vicinity of the diamagnetic transition but at a higher temperature (for $x=0.5$, $T_{\rho=0}=1$ K). In contrast to CeIrIn_5 , in which there is no pronounced ac-susceptibility signature when the resistivity vanishes, a weak diamagnetic response is observed in χ_{ac} at $T_{\rho=0}$ in $\text{CeRh}_{0.5}\text{Ir}_{0.5}\text{In}_5$ (Fig. 4).

For $x > 0.6$, ordered magnetism is completely suppressed and only a superconducting ground state is observed. Viewing this part of the phase diagram from the perspective of Rh-doping CeIrIn_5 reveals several remarkable features. At low Rh concentrations, T_c appears to decrease with increasing Rh concentration, which is the conventional expectation, but then, in the vicinity of $x \sim 0.9$, T_c recovers and increases with increasing Rh concentration. This feature in T_c versus x for $x \sim 0.9$ is reminiscent of what is observed for the pressure dependence of T_c in superconducting CeRhIn_5 .¹⁸ In addition to the bulk phase transition observed by heat capacity, a transition to zero resistance persists over a wide range of doping. $T_{\rho=0}$ is relatively independent of doping so that T_c approaches $T_{\rho=0}$ in the vicinity of $x=0.5$, resulting in a value of T_c that is more than double that of stoichiometric CeIrIn_5 . The upper critical field deduced from heat capacity measurements also increases significantly for $x \sim 0.5$ ($H_{c2}=3$ T compared with 0.5 T for CeIrIn_5), approaching values comparable to those required to produce a finite resistivity (5 T) in CeIrIn_5 .¹⁰

The remarkably rich phase diagram of $\text{CeRh}_{1-x}\text{Ir}_x\text{In}_5$ reflects the inherent “tunability” of ground states allowed by alternating $\text{CeIn}_3:\text{MIn}_2$ layers in CeMIn_5 .¹¹ This behavior is not limited to $\text{CeRh}_{1-x}\text{Ir}_x\text{In}_5$. Both $\text{CeRh}_{1-x}\text{Co}_x\text{In}_5$ and $\text{CeCo}_{1-x}\text{In}_x\text{In}_5$, although studied in less detail, show a similar multiplicity of phase transitions.¹⁹ In the case of CeRhIn_5 , the evolution from antiferromagnetic to superconducting ground state with pressure could be understood semiquanti-

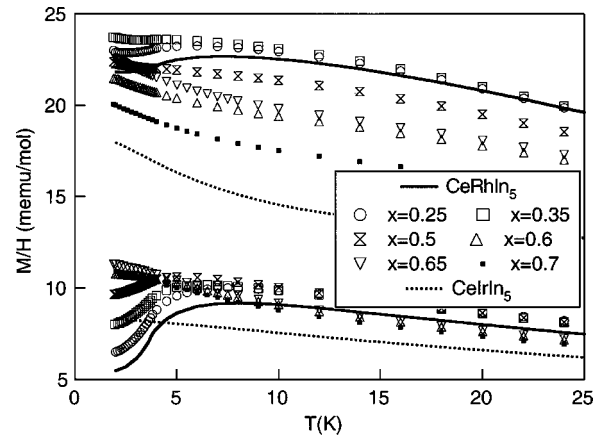


FIG. 5. Anisotropic magnetic susceptibility for representative x in $\text{CeRh}_{1-x}\text{Ir}_x\text{In}_5$. The upper (lower) cluster of curves are for $H \parallel c$ ($H \parallel a$).

tatively by considering the RhIn_2 layer as a source of chemical pressure on the CeIn_3 layer.⁸ The similarity of the T - P phase diagram of CeRhIn_5 to the x dependence of T_N in $\text{CeRh}_{1-x}\text{Ir}_x\text{In}_5$ suggests that the addition of Ir may act as an applied pressure. However, the in-plane lattice constant (which shrinks as a function of pressure) actually increases with increasing Ir concentration. Thus, “hydrostatic chemical pressure” would appear to be an inadequate explanation of the observed similarities. On the other hand, “uniaxial chemical pressure” appears to play a significant role in $\text{CeRh}_{1-x}\text{Ir}_x\text{In}_5$. If one considers the two ambient-pressure, stoichiometric superconductors in this family of compounds, CeIrIn_5 (Ref. 10) and CeCoIn_5 ,¹¹ one observes not only a substantial difference in T_c (0.4 K vs 2.3 K) but also a significant difference in c/a , the ratio of the tetragonal lattice constants (1.610 vs 1.637). To the extent that a larger c/a implies greater anisotropy, larger T_c for larger c/a is consistent with recent theories of magnetically mediated superconductivity.²⁰ The remarkable observation for the present $\text{CeRh}_{1-x}\text{Ir}_x\text{In}_5$ results is that the T_c in $\text{CeRh}_{0.5}\text{Ir}_{0.5}\text{In}_5$ can be “predicted” based on the difference in c/a between $\text{CeRh}_{0.5}\text{Ir}_{0.5}\text{In}_5$ and CeIrIn_5 and the slope given by CeCoIn_5 and CeIrIn_5 (i.e., $0.8 \text{ K} = 0.4 \text{ K} + 0.006\{1.9 \text{ K}/0.027\}$).

The variation in c/a with Ir content, which to some extent must reflect changes in f -ligand hybridization, also produces trends in the magnetic susceptibility that correlate with the ground state configuration. Figure 5 shows the anisotropic magnetic susceptibility for $2 \text{ K} < T < 25 \text{ K}$ for representative x in $\text{CeRh}_{1-x}\text{Ir}_x\text{In}_5$. χ_c , the susceptibility for field applied along the c axis, and χ_a , the susceptibility for field applied along the a axis, each reveal characteristic evolutions in T dependence that coincide with different regions of the x - T phase diagram. With increasing x , the maximum in χ_c near 7 K, which can be associated with two-dimensional (2D) magnetic fluctuations (and occurs above T_N),⁸ is suppressed and evolves into a Curie-like increase. The maximum in $\chi_c(T)$ disappears [i.e., $\chi_c(7 \text{ K}) \sim \chi_c(2 \text{ K})$] for $x \sim 0.4$, near the concentration at which superconductivity is first observed. The magnitude of $\chi_c(7 \text{ K})$ also reaches a maximum in this range. Thus, it appears that the spin environment/fluctuation spec-

trum that influences χ_c in these materials is coupled to superconductivity and is reminiscent of a broader trend observed in other CeMIn₅ compounds.¹¹ Accompanying these changes in χ_c is a corresponding evolution in $\chi_a(T)$: the loss of a maximum and subsequent drop in magnitude of susceptibility is centered around $x \sim 0.6$, the concentration at which magnetic order is lost. The greater sensitivity of $\chi_a(T)$ to magnetic order is consistent with the a axis being the easy magnetic direction.^{13,14} Thus, even at temperatures greater than the respective phase transitions, $\chi_c(T)$ signals the onset of superconductivity; whereas $\chi_a(T)$ reveals the loss of magnetism.

As discussed above, the coexistence of magnetism and superconductivity, rather than their competition, appears to be the rule and not the exception for U-based heavy fermion superconductors. CeRh_{1-x}Ir_xIn₅ clearly shares this feature. Preliminary photoemission data suggest another U-like characteristic of these materials.²¹ Despite the observed large values of γ , no suggestion of a “Kondo resonance” near the Fermi surface is observed in these materials. Furthermore, local-density-approximation band structure calculations—which neglect many-body correlation effects—do a surprisingly good job of describing the electronic properties of CeMIn₅.^{22,23} It would appear, then, that the relevant f -spectral weight may be more bandlike than localized, and

perhaps such a situation is more susceptible to the coexistence of magnetism and superconductivity. Unfortunately, much of our present intuition derives from the localized limit.²⁴ Thus, the CeMIn₅ materials and CeRh_{1-x}Ir_xIn₅ in particular may provide an opportunity to bridge our understanding of U-based and Ce-based heavy fermion superconductivity.

In summary, we have presented a phase diagram for CeRh_{1-x}Ir_xIn₅ that reveals several remarkable features. Superconductivity is observed over a very broad range of doping, $0.3 < x \leq 1$, including a substantial range ($0.3 < x < 0.6$) over which it coexists with long-range magnetic order. The zero-resistance transition observed in stoichiometric CeIrIn₅ is robust against Rh substitution. In fact, the bulk T_c more than doubles by CeRh_{0.5}Ir_{0.5}In₅, approaching the relatively unchanged zero-resistance transition temperature. The ground state evolution with Ir substitution appears to be “controlled” by changes in c/a , reflective of variations in f -ligand hybridization.

We thank N.J. Curro for valuable discussions. Work at Los Alamos was performed under the auspices of the U.S. Department of Energy. Z.F. and P.G.P. acknowledge partial support from the N.S.F. (Grant Nos. DMR-9870034 and DMR-9971348), and FAPESP (Grant No. 9901062-0).

¹See, e.g., M. Tinkham, *Introduction to Superconductivity* (McGraw-Hill, New York, 1975).

²M. B. Maple, *J. Alloys Compd.* **303**, 1 (2000).

³N. D. Mathur *et al.*, *Nature (London)* **394**, 39 (1998).

⁴R. H. Heffner and M. R. Norman, *Comments Condens. Matter Phys.* **17**, 361 (1996).

⁵P. Gegenwart *et al.*, *Phys. Rev. Lett.* **81**, 1501 (1998).

⁶For a recent counter-argument, see F. M. Grosche *et al.*, *cond-mat/0012118* (unpublished).

⁷N. Grewe and F. Steglich, in *Handbook on the Chemistry and Physics of Rare Earths*, edited by K. A. Gschneidner and L. Eyring, Vol. 14 (North-Holland, Amsterdam, 1991), p. 343.

⁸H. Hegger *et al.*, *Phys. Rev. Lett.* **84**, 4986 (2000).

⁹J. D. Thompson *et al.*, *J. Magn. Magn. Mater.* **226**, 5 (2001).

¹⁰C. Petrovic *et al.*, *Europhys. Lett.* **53**, 354 (2001).

¹¹C. Petrovic *et al.*, *J. Phys.: Condens. Matter* **13**, L337 (2001).

¹²E. Moshopoulou *et al.*, *J. Solid State Chem.* **158**, 25 (2001).

¹³N. J. Curro *et al.*, *Phys. Rev. B* **62**, 6100 (2000).

¹⁴W. Bao *et al.*, *Phys. Rev. B* **62**, 14 621 (2000).

¹⁵P. G. Pagliuso *et al.* (unpublished).

¹⁶R. Movshovich *et al.*, *Phys. Rev. Lett.* **86**, 5152 (2001).

¹⁷R. H. Heffner *et al.* (unpublished); neutron diffraction measurements confirm that this static magnetization results from an ordered magnetic structure similar to that of CeRhIn₅ [W. Bao *et al.* (unpublished)].

¹⁸T. Muramatsu *et al.* (unpublished).

¹⁹P. G. Pagliuso *et al.*, *cond-mat/0107266* (unpublished).

²⁰P. Monthoux and G. G. Lonzarich, *Phys. Rev. B* **63**, 054529 (2001).

²¹J. J. Joyce *et al.* (unpublished).

²²Y. Haga *et al.*, *Phys. Rev. B* **63**, 060503 (2001).

²³D. Hall *et al.*, *Phys. Rev. B* **64**, 064506 (2001).

²⁴S. Doniach, in *Valence Instabilities and Related Narrow Band Phenomena*, edited by R. D. Parks (Plenum, New York, 1977), p. 169.